Eur. Phys. J. A **24**, 39–49 (2005)
DOI 10.1140/epja/i2004-10119-4

THE EUROPEAN PHYSICAL JOURNAL A

High-spin structures of $^{121,123,125,127}_{51}$Sb nuclei: Single proton and core-coupled states

M.-G. Porquet[1,a], Ts. Venkova[2], R. Lucas[3], A. Astier[4,1], A. Bauchet[1], I. Deloncle[1], A. Prévost[4,1], F. Azaiez[5,b], G. Barreau[6], A. Bogachev[7], N. Buforn[4], A. Buta[5], D. Curien[5], T.P. Doan[6], L. Donadille[8,3], O. Dorvaux[5], G. Duchêne[5], J. Durell[9], Th. Ethvignot[10], B.P.J. Gall[5], D. Grimwood[9], M. Houry[3,c], F. Khalfallah[5], W. Korten[3], S. Lalkovski[11], Y. Le Coz[3], M. Meyer[4], A. Minkova[11], I. Piqueras[5], N. Redon[4], A. Roach[9], M. Rousseau[5], N. Schulz[5], A.G. Smith[9], O. Stézowski[4], Ch. Theisen[3], and B.J. Varley[9]

[1] CSNSM IN2P3-CNRS and Université Paris-Sud, 91405 Orsay, France
[2] INRNE, BAS, 1784 Sofia, Bulgaria
[3] Commissariat à l'Energie Atomique, CEA/Saclay, DSM/DAPNIA/SPhN, 91191 Gif-sur-Yvette Cedex, France
[4] IPNL, IN2P3-CNRS and Université Claude Bernard, 69622 Villeurbanne Cedex, France
[5] IReS, IN2P3-CNRS and Université Louis Pasteur, 67037 Strasbourg Cedex 2, France
[6] CENBG, IN2P3-CNRS and Université Bordeaux I, 33175 Gradignan, France
[7] JINR, Joliot-Curie 6, 141980, Dubna, Moscow region, Russia
[8] School of Physics and Astronomy, University of Birmingham, Birmingham, B15 2TT, UK
[9] Department of Physics and Astronomy, University of Manchester, Manchester, M13 9PL, UK
[10] Commissariat à l'Energie Atomique, CEA/DIF/DPTA, Service de Physique Nucléaire, B.P. 12, 91680 Bruyères-le-Châtel, France
[11] University of Sofia, Faculty of Physics, 1126 Sofia, Bulgaria

Received: 26 October 2004 / Revised version: 16 December 2004 /
Published online: 24 January 2005 –
Communicated by D. Schwalm

Abstract. The ^{121,123,125,127}Sb nuclei have been produced as fission fragments in three reactions induced by heavy ions: ^{12}C + ^{238}U at 90 MeV bombarding energy, ^{18}O + ^{208}Pb at 85 MeV, and ^{31}P + ^{176}Yb at 152 MeV. Their level schemes have been built from gamma rays detected using the EUROBALL III and IV arrays. High-spin states of ^{123,125,127}Sb nuclei have been identified for the first time. Moreover isomeric states lying around 2.3 MeV have been established in ^{123,125,127}Sb from the delayed coincidences between the fission fragment detector SAPhIR and the gamma array. All the observed states can be described by coupling a $d_{5/2}$ or $g_{7/2}$ proton to an excited Sn core involving either vibrational states or broken neutron pairs.

PACS. 21.60.Ev Collective models – 23.20.Lv γ transitions and level energies – 25.85.Ge Charged-particle-induced fission – 27.60.+j $90 \leq A \leq 149$

1 Introduction

The light-mass $_{51}$Sb isotopes have been largely studied at high angular momenta from fusion-evaporation reactions, many years ago. Their level schemes have first revealed the rotational structures built on the $\pi 9/2^+[404]$ orbit, originating from a one-hole two-particle excitation across the $Z = 50$ gap, coexisting with the normal states, one proton coupled to the spherical Sn core [1,2]. In the Sn isotopes, the excitations across the $Z = 50$ gap have been also identified. Quasi-rotational bands, which are yrast at spin values around $6\hbar$ in $^{112-118}$Sn isotopes, are built on two-hole two-particle states [3]. Later on, a lot of rotational bands corresponding to this 2h-2p core excitation have been identified at very high spin in the $^{109-119}$Sb isotopes, the supplementary odd proton being for instance located in the $\pi h_{11/2}$ orbital, well lowered in energy because of the deformation [4–8].

Whereas these 2h-3p excitations dominate the very high-spin structures of the $^{109-119}$Sb isotopes, they are no longer expected to be observed in the heavy masses since

[a] e-mail: porquet@csnsm.in2p3.fr
[b] *Present address*: IPN, IN2P3-CNRS and Université Paris-Sud, 91406 Orsay, France.
[c] *Present address*: Commissariat à l'Energie Atomique, CEA/DIF/DRCE, Service Diagnostiques Expérimentaux, B.P. 12, 91680 Bruyères-le-Châtel, France.

the excitation energies of all these deformed structures evolve with the neutron number showing a minimum at the middle of the $N = 50$–82 shell ($N \sim 66$). Therefore the yrast decays of the unknown high-spin states of $^{123-127}$Sb would only show the spherical states corresponding to the coupling of one proton to the Sn core excitation, particularly the broken neutron pairs. Such states are very interesting as they give access to the values of the residual interaction between proton and neutron located in different sub-shells, which are needed for the shell model calculations. Unfortunately, the high-spin level schemes of the heavy Sb isotopes cannot be populated via the usual fusion-evaporation reactions because of the lack of suitable stable projectile-target combinations.

Such a work has been recently undertaken thanks to the fission of actinides induced by neutrons and the spontaneous fission of ^{248}Cm. Several high-spin states have been measured in ^{129,131}Sb [9,10] and in ^{133}Sb [11], respectively.

For the study presented in this paper, the $^{119-127}$Sb isotopes have been produced as fragments of binary fission induced by heavy ions. We have selected three fusion reactions in order to get a large number of Sb isotopes, from the stability line to the most neutron-rich nuclei as possible. High-spin states of ^{123,125,127}Sb nuclei have been identified for the first time. Moreover, new isomeric states lying around 2.3 MeV have been established in these three Sb isotopes from the delayed coincidences between fission fragment detectors and the gamma array. All the observed states can be described by coupling a $d_{5/2}$ or $g_{7/2}$ proton to an excited $_{50}$Sn core involving either vibrational states (2^+, 4^+, and 3^-) or broken neutron pairs from $\nu h_{11/2}$ and several $N = 4$ neutron sub-shells.

2 Experimental procedures and data analysis

2.1 Reactions and γ-ray detection

The ^{12}C + ^{238}U reaction was studied at 90 MeV incident energy. The beam was provided by the Legnaro XTU tandem accelerator. A 47 mg/cm^2 target of ^{238}U was used to stop the recoiling nuclei. The gamma rays were detected with the EUROBALL III array [12]. The spectrometer contained 15 Cluster germanium detectors placed in the backward hemisphere with respect to the beam, 26 Clover germanium detectors located around 90°, and 30 tapered single-crystal germanium detectors located at forward angles. Each Cluster detector consists of seven closely packed large-volume Ge crystals [13] and each Clover detector consists of four smaller Ge crystals [14]. The data were recorded in an event-by-event mode with the requirement that a minimum of five unsuppressed Ge detectors fired in prompt coincidence. About 1.9×10^9 coincidence events with a γ multiplicity greater than or equal to three were registered. Events were sorted by the EURO14 software [15] and analysed with the Radware package [16].

The second and third reactions were studied at the Vivitron accelerator of IReS (Strasbourg), using the EUROBALL IV spectrometer which consists of the same array of Ge crystals as EUROBALL III and an inner ball of 210 BGO crystals. For the fusion reaction, ^{18}O + ^{208}Pb at 85 MeV beam energy, the thickness of the target was 100 mg/cm^2. The third fusion reaction was ^{31}P + ^{176}Yb at 145 MeV beam energy. The 1.5 mg/cm^2 target was deposited in a 15 mg/cm^2 Au backing in order to stop the recoiling nuclei. With the requirement of a minimum of three unsuppressed Ge detectors firing in prompt coincidence, a total of 4×10^9 and 2.2×10^9 coincidence events were collected in the ^{18}O and ^{31}P induced reactions, respectively. The offline analysis consisted of both usual γ-γ sorting and multi-gated spectra using the FANTASTIC software [17] and several three-dimensional "cubes" built and analysed with the Radware package [16].

2.2 Isomer selection

To identify new isomeric states in fission fragments, we have performed another experiment using a fission fragment detector to trigger the EUROBALL III array and isolate the delayed γ-ray cascades. The heavy-ion detector, SAPhIR, is made of many photovoltaic cells which can be arranged in several geometries [18]. In the present work, it consisted of 32 photovoltaic modules laying in four rings around the target. We have used the ^{12}C + ^{238}U reaction at 90 MeV with a thin target, 0.14 mg/cm^2. Fragments escaping from the target are stopped in the photovoltaic cells of SAPhIR. The detection of the two fragments in coincidence provides a clean signature of fission events. The EUROBALL III time window was 1 μs, allowing detection of delayed γ-rays emitted during the de-excitation of isomeric states.

Time spectra between fragments and γ-rays have been analyzed in order to measure the half-life of isomeric levels. The FWHM of the time distribution for prompt γ-rays was around 15 ns. In this experiment, new isomeric states have been found in ^{123,125,127}Sb nuclei, which will be detailed below.

2.3 Identification of new γ-ray cascades

More than one hundred nuclei are produced at high spin in such experiments, and this gives several thousands of γ transitions which have to be sorted out. Single-gated spectra are useless in the majority of cases. The selection of one particular nucleus needs at least two energy conditions, implying that at least two transitions have to be known.

The identification of transitions depopulating high-spin levels which are completely unknown is based on the fact that prompt γ-rays emitted by complementary fragments are detected in coincidence [19,20]. For each reaction used in this work, we have studied many pairs of complementary fragments with known γ-ray cascades to establish the relationship between their number of protons and neutrons. The sum of the proton numbers of complementary fragments has been found to be always the atomic number of the compound nucleus. The total number of evaporated neutrons (sum of the pre- and post-fission emitted neutrons) is mainly 10 in the ^{12}C + ^{238}U reaction [21,22], and 6 in the two other reactions [23,24]. These

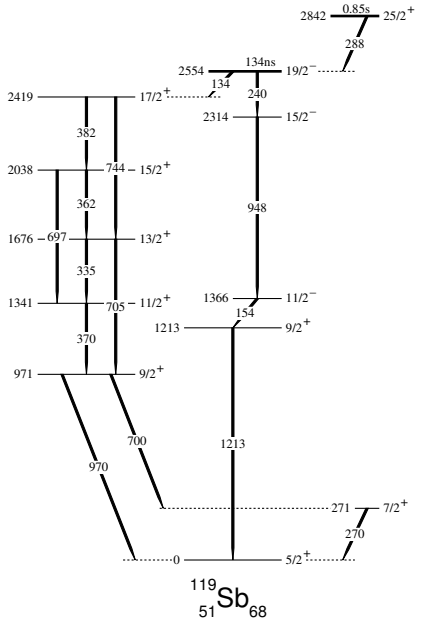

Fig. 1. Level scheme of ^{119}Sb obtained as a fission fragment in the fusion reaction ^{31}P + ^{176}Yb at 152 MeV beam energy.

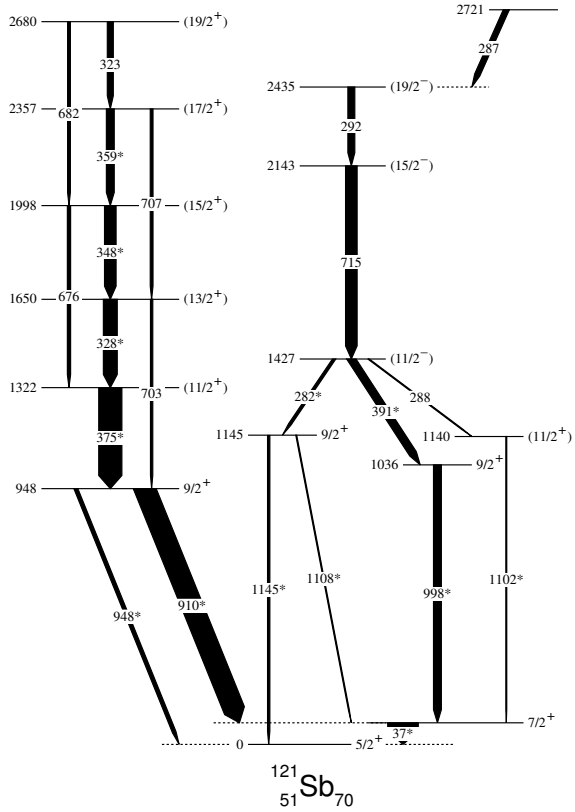

Fig. 2. Level scheme of ^{121}Sb obtained as a fission fragment in the fusion reaction ^{31}P + ^{176}Yb at 152 MeV beam energy. The transitions marked with a star were already known [27]. The level at 2721 keV excitation energy can be the expected long-lived isomeric state with spin $25/2^+$ (see text).

numbers have been used to identify the γ-ray cascades of ^{123,125,127}Sb nuclei, as explained in the next section.

Finally, the use of different reactions to produce the various Sb isotopes has turned out to be very efficient to disentangle the coincidence relationships which are often complicated by the existence of many doublets or triplets of transitions very close in energy.

In fission experiments, spin values can be assigned on the basis of γ_1-γ_2 angular-correlation results [25]. The statistics of our data were unfortunately too poor to perform such a measurement in the Sb isotopes, as we need to select the nucleus by gating on the energy of a third transition (detected at any angle). Therefore, in this work, the spin assignments are based upon i) the already known spins of some states, ii) the assumption that in yrast decays, spin values increase with the excitation energy, iii) the analogy with the level structures of the lighter isotopes, iv) the possible existence of crossover transitions.

3 Experimental results

The $^{119-123}$Sb isotopes are produced as fission fragments of $_{85}$At isotopes obtained in the fusion reaction ^{31}P + ^{176}Yb at 152 MeV beam energy. The mass interval is shifted towards the heavy-mass side when using the two other reactions. Therefore, the high-spin states of the ^{125,127}Sb isotopes have been obtained from the analysis of the ^{18}O and ^{12}C induced reactions.

3.1 Study of ^{119,121}Sb

The high-spin states of ^{119}Sb observed in this work extend up to the 2842 keV level and are in complete agreement with those already known from fusion-evaporation reactions [26,8]. The level scheme of ^{119}Sb is shown in fig. 1 as it will be useful to discuss the new structures observed in ^{121}Sb. A very long-lived isomeric state, $T_{1/2} = 0.85$ s, had been measured in ^{119}Sb [1]. The large value of the total conversion coefficient of the 288 keV transition determined from intensity balance indicates a $M2$ or $E3$ character. Therefore, it has been assumed that the 2842 keV state with $I^\pi = 25/2^+$ is the isomeric level [26]. In ref. [8], the configuration of the 2842 keV state which is assigned to be $21/2^-$ is not discussed. Moreover, in this experiment, a lot of cascades are seen up to spin 31/2, whereas no level decaying into this $21/2^-$ state has been observed, even though it is yrast. This can be due to the long-lived isomeric state. Therefore, we have adopted the conclusion of ref. [26] for the assignment of the long-lived isomeric state of ^{119}Sb (see fig. 1).

The high-spin states of ^{121}Sb had been previously studied by means of a fusion-evaporation reaction [2]. A more complete level scheme has been deduced from the present experiment using the spectra gated by all the combinations of already known transitions and new ones identified in those spectra (see fig. 2). All the transitions assigned to ^{121}Sb are given in table 1. The strongly coupled rotational

Table 1. Properties of the transitions assigned to ^{121}Sb observed in this experiment.

$E_\gamma^{(a)}$	$I_\gamma^{(a)}$	$J_i \rightarrow J_f$	E_i	E_f
282.0(4)*	13(4)	$(11/2^-) \rightarrow 9/2^+$	1427.2	1144.8
286.5(4)	23(6)	$\rightarrow (19/2^-)$	2721.3	2434.8
288.0(5)	2.5(10)	$(11/2^-) \rightarrow 11/2^+$	1427.2	1139.5
292.2(4)	30(6)	$(19/2^-) \rightarrow (15/2^-)$	2434.8	2142.6
323.0(4)	27(7)	$(19/2^+) \rightarrow 17/2^+$	2680.4	2357.4
327.9(3)*	60(6)	$13/2^+ \rightarrow 11/2^+$	1650.3	1322.4
348.1(3)*	50(7)	$15/2^+ \rightarrow 13/2^+$	1998.4	1650.3
359.0(3)*	34(7)	$17/2^+ \rightarrow 15/2^+$	2357.4	1998.4
374.9(3)*	100(10)	$11/2^+ \rightarrow 9/2^+$	1322.4	947.5
391.4(3)*	34(6)	$(11/2^-) \rightarrow 9/2^+$	1427.2	1035.8
676.1(4)	15(5)	$15/2^+ \rightarrow 11/2^+$	1998.4	1322.4
682.3(4)	12(4)	$(19/2^+) \rightarrow 15/2^+$	2680.4	1998.4
702.5(4)	10(3)	$13/2^+ \rightarrow 9/2^+$	1650.3	947.5
707.0(4)	13(4)	$17/2^+ \rightarrow 13/2^+$	2357.4	1650.3
715.4(3)	50(7)	$(15/2^-) \rightarrow (11/2^-)$	2142.6	1427.2
910.0(5)*	93(10)	$9/2^+ \rightarrow 7/2^+$	947.5	37.5
948.3(5)*	17(4)	$9/2^+ \rightarrow 5/2^+$	947.5	0.0
998.3(3)*	34(6)	$9/2^+ \rightarrow 7/2^+$	1035.8	37.5
1102.0(5)*	2.5(10)	$11/2^+ \rightarrow 7/2^+$	1139.5	37.5
1107.5(4)*	3.5(10)	$9/2^+ \rightarrow 7/2^+$	1144.8	37.5
1144.7(3)*	10(2)	$9/2^+ \rightarrow 5/2^+$	1144.8	0.0

(a) The number in parenthesis is the error in the last digit, the transitions marked with a star were already known [27].

Table 2. Properties of the transitions assigned to ^{123}Sb observed in this experiment.

$E_\gamma^{(a)}$	$I_\gamma^{(a)}$	$J_i \rightarrow J_f$	E_i	E_f
127.0(5)	5(2)	$(21/2^+) \rightarrow (19/2^+)$	2612.7	2485.7
160.1(2)*	15(4)	$5/2^+ \rightarrow 7/2^+$	160.1	0.0
200.4(2)	73(15)	$(19/2^-) \rightarrow (15/2^-)$	2237.2	2036.8
238.5(3)	12(4)	$(27/2^-) \rightarrow (25/2^-)$	4024.4	3785.9
367.4(4)	11(4)	$\rightarrow (27/2^-)$	4391.8	4024.4
380.3(4)	11(4)		4772.1	4391.8
381.0(2)	100(15)	$(15/2^-) \rightarrow (11/2^-)$	2036.8	1655.8
395.2(2)	22(5)	$(11/2^-) \rightarrow 9/2^+$	1655.8	1260.4
438.1(3)	12(4)	$(25/2^-) \rightarrow (23/2^-)$	3785.9	3347.8
441.7(4)	12(4)	$(19/2^+) \rightarrow (15/2^+)$	2485.7	2044.0
482.0(5)	3(1)	$(23/2^+) \rightarrow (19/2^+)$	2967.7	2485.7
497.2(3)	19(5)	$(21/2^-) \rightarrow (19/2^-)$	2734.4	2237.2
567.3(3)	12(3)	$(11/2^-) \rightarrow 11/2^+$	1655.8	1088.6
613.4(3)	12(3)	$(23/2^-) \rightarrow (21/2^-)$	3347.8	2734.4
625.7(3)	63(12)	$(11/2^-) \rightarrow 11/2^+$	1655.8	1030.1
676.8(5)	6(3)	$(27/2^-) \rightarrow (23/2^-)$	4024.4	3347.8
955.4(3)	25(6)	$(15/2^+) \rightarrow 11/2^+$	2044.0	1088.6
1030.1(3)*	63(9)	$9/2^+ \rightarrow 7/2^+$	1030.1	0.0
1088.6(3)*	37(5)	$11/2^+ \rightarrow 7/2^+$	1088.6	0.0
1100.2(3)*	15(4)	$9/2^+ \rightarrow 5/2^+$	1260.4	160.1
1110.8(4)	13(4)	$(23/2^-) \rightarrow (19/2^-)$	3347.8	2237.2
1260.5(4)*	7(2)	$9/2^+ \rightarrow 7/2^+$	1260.4	0.0

(a) The number in parenthesis is the error in the last digit, the transitions marked with a star were already known [28].

band built on the $9/2^+[404]$ level has been extended by one transition and all the crossover transitions have been observed for the first time in this experiment. Moreover, a new sequence of three transitions (287, 292 and 715 keV) has been measured in coincidence with the five transitions depopulating the 1427 keV level which was known from β-decay measurement [27]. An $11/2^-$ spin value can be assigned to this state as it is also populated with $L = 3$ in the (p, t) reaction [27]. Such a value is consistent with its population in this experiment and with its decays towards the two $9/2^+$ states at 1036 keV and 1145 keV. We have observed a new decay branch towards the 1140 keV state, which can be assigned as a $11/2^+$ state. The 287-292-715 cascade that we have placed above the $(11/2^-)$ state, is very similar to the 288-240-948 cascade located between the long-lived $25/2^+$ isomeric state and the $11/2^-$ state in ^{119}Sb (see fig. 1). Moreover, another indication of the decay of a long-lived isomeric state is the fact that we could not observe any transition located above the 2721 keV level, although the available number of counts would have allowed us to observe a higher-spin part of the cascade. Therefore, we propose that the 2721 keV level in ^{121}Sb is the $25/2^+$ state expected in this energy range, similar to the one already measured in ^{117,119}Sb [26].

3.2 Study of ^{123}Sb

Very few high-spin levels were known in the stable ^{123}Sb isotope prior to this work. From the β-decay of the $11/2^-$ ground state of ^{123}Sn and Coulomb excitation experiment [28], the 1030 keV and 1089 keV levels had been assigned as $9/2^+$ and $(9/2^+, 11/2^+)$, respectively. Using the data of the fusion-fission reaction ^{12}C + ^{238}U, we have looked for the ^{123}Sb transitions using spectra gated by the first transitions of its main complementary fragments, ^{115,116}Ag [23,29]. Besides the other γ-lines belonging to the Ag isotopes, these spectra also exhibit the 1030 and 1089 keV transitions which are assigned to ^{123}Sb. Then two new transitions (626 and 381 keV) have been clearly seen in the spectra in double coincidence with the 1030 keV transition and the 125 keV transition (belonging to both Ag isotopes). All the double-gated γ-ray spectra with gates on the 1030, 626 and 381 keV transitions have been used to identify other new transitions. Finally, their mutual coincidences, cross-checked in the data sets from the three fusion-fission reactions, have allowed us to establish the level scheme shown in fig. 3. All the transitions assigned to ^{123}Sb are given in table 2.

The decay of the 1656 keV level populates the three medium-spin levels located around 1 MeV excitation energy, known from the β-decay of the $11/2^-$ ground state of ^{123}Sn and from Coulomb excitation [28]. A $11/2^-$ spin value is assigned to this state because of its decay, which is similar to the one of the $11/2^-$ state of the lighter isotopes (see figs. 1 and 2). Moreover, we assume that the 1656 keV level measured in the present work is the same as the one located at 1644 ± 10 keV which had been populated with $L = 5$ in stripping reaction [28]. The states at 3786 and 4392 keV are drawn with dashed lines because

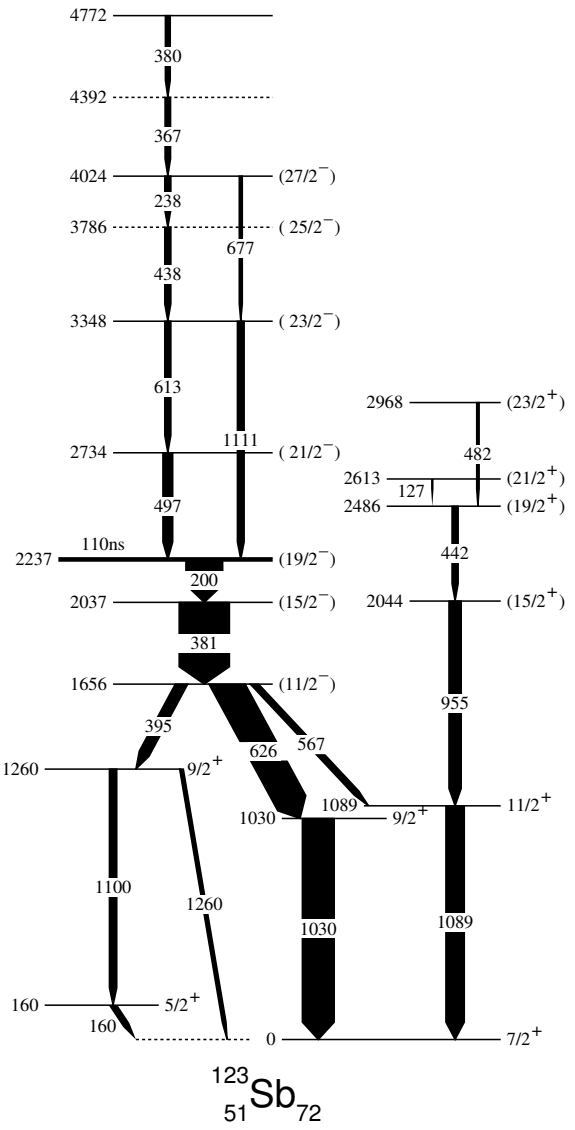

Fig. 3. Level scheme of ^{123}Sb deduced in the present work. The spin and parity values given without parenthesis have been determined from β-decay measurements [28]. The $(19/2^-)$ level at 2237 keV excitation energy is isomeric, $T_{1/2} = 110 \pm 10$ ns. Two levels are drawn with dashed lines because the order of some coincident transitions having similar intensities could not be unambiguously established.

the order of the gamma transitions (438 and 238 keV, 367 and 380 keV) cannot be precisely determined, their relative intensities being very close.

The analysis of delayed γ-rays in the experiment triggered by the SAPhIR fission-fragment detector has revealed the existence of an isomeric state in ^{123}Sb. One example of the delayed spectra is given in fig. 4. All the transitions involved in the decay of the 2237 keV level are observed in these data. Its half-life was measured to be 110 ± 10 ns: an $E2$ multipolarity for the 200 keV transition can account for such a value (the calculated reduced transition probability being 0.4 W.u.). This transition has

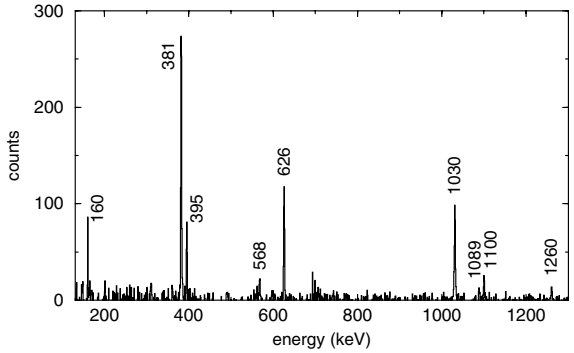

Fig. 4. Spectrum of γ-rays which have been detected in the time interval 50 ns–1 μs after the detection of two fragments by SAPhIR and in prompt coincidence with the 200 keV transition, showing all the delayed transitions emitted by ^{123}Sb.

been assigned as $(19/2^-) \rightarrow (15/2^-)$, from the analogy with ^{119,121}Sb.

It is worth pointing out that the high-spin level scheme of ^{123}Sb displays large changes as compared to the lighter isotopes. The collective band built on the $9/2^+[404]$ intruder state (located at 1337 keV excitation energy) is no longer observed. Even the first member of the band already known from the (^{7}Li, α2n) reaction [2] has not been populated. This is mainly due to the fact that the band-head state is too high in energy in this isotope as compared to ^{119,121}Sb, where the excitation energy of the intruder state is minimum [2] (middle of the N = 50–82 neutron shell).

3.3 Study of ^{125}Sb

The high-spin states of ^{125}Sb have been studied from the data of the two reactions ^{12}C + ^{238}U and ^{18}O + ^{208}Pb. Starting from the first $11/2^+$ state known at 1089 keV [30], we have used the same method as described in the previous subsection in order to identify the main transitions populating the $11/2^+$ state. In the data from the ^{12}C + ^{238}U reaction, the 1089 keV transition is observed in the spectrum gated by the two first transitions (125 and 636 keV) of ^{115}Ag [23,31], the main complementary fragment of ^{125}Sb. Then four new transitions (132, 331, 904 and 1103 keV) are identified in the spectra in double coincidence with the 1089 keV transition and the 125 keV or the 636 keV transition. These new transitions are also confirmed in the data from the ^{18}O + ^{208}Pb reaction, being in coincidence with those of ^{95}Y [32], the main complementary fragment of ^{125}Sb. The analysis of all the coincidence relationships has led to the level scheme drawn in fig. 5. All the transitions assigned to ^{125}Sb are given in table 3.

Using the data from the SAPhIR experiment, the six transitions involved in the de-excitation of the 2470 keV level have been found to be delayed, corresponding to the decay of an isomeric state with $T_{1/2} = 155 \pm 20$ ns (fig. 6). An $E2$ multipolarity for the 146 keV transition can account for such a value and the isomeric state has been

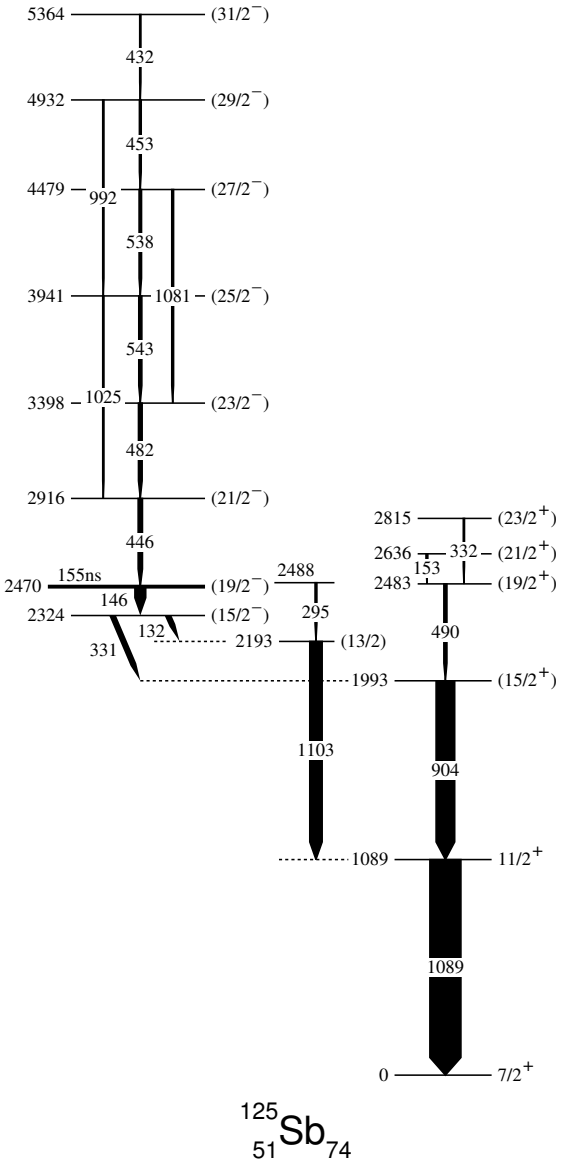

Fig. 5. Level scheme of ^{125}Sb deduced in the present work. The spin and parity values given without parenthesis have been established from previous measurements [30]. The $(19/2^-)$ level at 2470 keV excitation energy is isomeric, $T_{1/2} = 155 \pm 20$ ns.

Table 3. Properties of the transitions assigned to ^{125}Sb observed in this experiment.

$E_\gamma^{(a)}$	$I_\gamma^{(a)}$	$J_i \rightarrow J_f$	E_i	E_f
131.5(2)	32(6)	$(15/2^-) \rightarrow (13/2)$	2324.2	2192.6
145.9(2)	65(10)	$(19/2^-) \rightarrow (15/2^-)$	2470.1	2324.2
152.7(3)	9(3)	$(21/2^+) \rightarrow (19/2^+)$	2636.1	2483.4
295.1(4)	5(1)	$\rightarrow (13/2)$	2487.7	2192.6
331.1(4)	32(7)	$(15/2^-) \rightarrow (15/2^+)$	2324.2	1993.2
331.6(4)	4(2)	$(23/2^+) \rightarrow (19/2^+)$	2815.0	2483.4
432.0(5)	2.6(8)	$(31/2^-) \rightarrow (29/2^-)$	5363.7	4931.7
446.3(3)	20(4)	$(21/2^-) \rightarrow (19/2^-)$	2916.4	2470.1
452.9(5)	4(1)	$(29/2^-) \rightarrow (27/2^-)$	4931.7	4478.8
481.8(3)	12(2)	$(23/2^-) \rightarrow (21/2^-)$	3398.2	2916.4
490.2(3)	16(3)	$(19/2^+) \rightarrow (15/2^+)$	2483.4	1993.2
538.1(4)	5.0(15)	$(27/2^-) \rightarrow (25/2^-)$	4478.8	3940.7
542.5(3)	9(3)	$(25/2^-) \rightarrow (23/2^-)$	3940.7	3398.2
903.8(3)	100(10)	$(15/2^+) \rightarrow 11/2^+$	1993.2	1089.4
991.5(5)	1.5(6)	$(29/2^-) \rightarrow (25/2^-)$	4931.7	3940.7
1024.7(5)	2.0(7)	$(25/2^-) \rightarrow (21/2^-)$	3940.7	2916.4
1080.5(5)	3(1)	$(27/2^-) \rightarrow (23/2^-)$	4478.8	3398.2
1089.4(3)*	–	$11/2^+ \rightarrow 7/2^+$	1089.4	0.0
1103.2(3)	70(8)	$(13/2) \rightarrow (11/2^+)$	2192.6	1089.4

(a) The number in parenthesis is the error in the last digit, the transition marked with a star was already known [30].

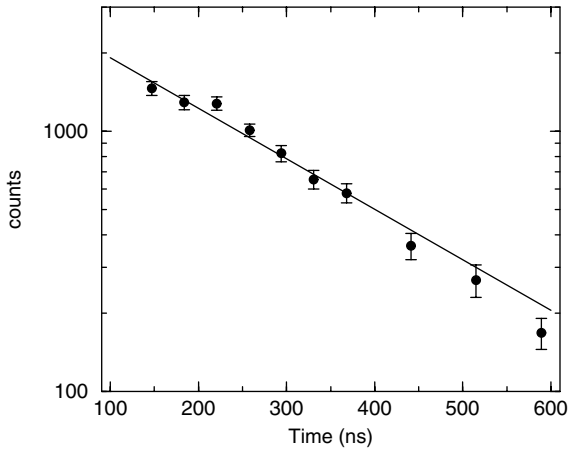

Fig. 6. Decay curve of the 331 keV transition of ^{125}Sb produced as a fission fragment from the ^{12}C + ^{238}U reaction. The straight line corresponds to a half-life of 155 ns.

assigned to be $(19/2^-)$, as in ^{123}Sb. One can remark that the decay of the $(15/2^-)$ state is not the same as the one measured in the lighter isotopes, the $(11/2^-)$ state located at 1889.9 keV being not populated, while it is very similar to the 1656 keV state of ^{123}Sb (they are both populated with $L = 5$ in stripping reactions [28,30]).

3.4 Study of ^{127}Sb

The study of the β-decay of ^{127}Sn^g ($I^\pi = 11/2^-$) has led to the identification of two $(11/2^+, 9/2^+)$ levels at 1096 and 1114 keV excitation energies in ^{127}Sb [33,34]. They directly decay to the $7/2^+$ ground state. We have looked for the 1096 and 1114 keV gamma rays in the spectra gated by the two first transitions of its two main complementary fragments, which are, respectively, ^{94}Y in the O + Pb reaction and ^{113}Ag in the C + U reaction. Only the 1096 keV is observed in these two spectra. Then new transitions have been identified in the spectra in double coincidence with the 1096 keV gamma line and a transition of ^{94}Y [32] or ^{113}Ag [31], they are assigned to ^{127}Sb. These new transitions have been used for further investigations of the coincidence data in order to establish the level scheme shown in fig. 7. All the transitions assigned to ^{127}Sb are given in table 4 and an example of double-gated spectra is given in fig. 8.

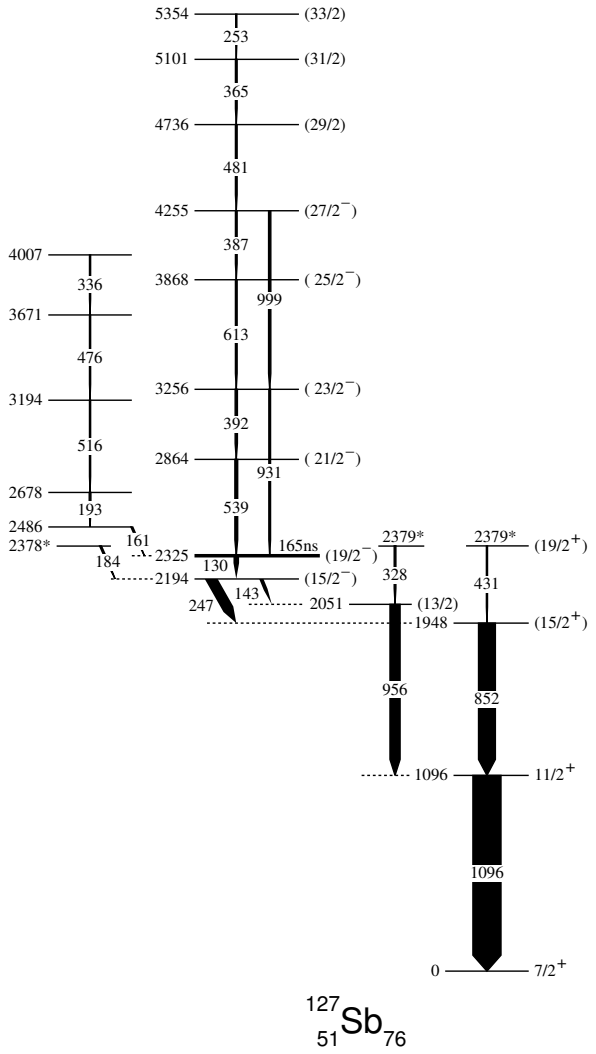

Fig. 7. Level scheme of ^{127}Sb deduced in the present work. The spin and parity values given without parenthesis have been established from previous measurements [33]. The exact number of the levels located between 2378 and 2379 keV is uncertain (see text): their energy is written with a star. The $(19/2^-)$ level is isomeric, $T_{1/2} = 165 \pm 20$ ns.

Table 4. Properties of the transitions assigned to ^{127}Sb observed in this experiment.

$E_\gamma^{(a)}$	$I_\gamma^{(a)}$	$J_i \rightarrow J_f$	E_i	E_f
130.4(2)	31(7)	$(19/2^-) \rightarrow (15/2^-)$	2324.8	2194.4
143.2(2)	20(5)	$(15/2^-) \rightarrow (13/2)$	2194.4	2051.1
160.8(3)	8(2)	$\rightarrow (19/2^-)$	2485.6	2324.8
183.7(4)	8(2)	$\rightarrow (15/2^-)$	2378.1	2194.4
192.6(4)	3.8(11)		2678.2	2485.6
246.9(2)	61(9)	$(15/2^-) \rightarrow (15/2^+)$	2194.4	1947.6
252.8(4)	3.1(12)	$(33/2) \rightarrow (31/2)$	5354.2	5101.4
328.0(3)	9(2)	$\rightarrow (13/2)$	2379.1	2051.1
336.4(5)	1.3(5)		4007.1	3670.7
365.4(4)	4.6(12)	$(31/2) \rightarrow (29/2)$	5101.4	4736.0
386.6(4)	5.4(15)	$(27/2^-) \rightarrow (25/2^-)$	4254.7	3868.1
391.8(4)	11(3)	$(23/2^-) \rightarrow (21/2^-)$	3255.5	2863.7
431.1(5)	1.5(5)	$(19/2^+) \rightarrow (15/2^+)$	2378.7	1947.6
476.3(5)	1.5(5)		3670.7	3194.4
481.3(4)	4.6(13)	$(29/2) \rightarrow (27/2^-)$	4736.0	4254.7
516.2(5)	3.1(9)		3194.4	2678.2
538.9(3)	15(4)	$(21/2^-) \rightarrow (19/2^-)$	2863.7	2324.8
612.6(4)	8(2)	$(25/2^-) \rightarrow (23/2^-)$	3868.1	3255.5
852.0(2)	100(10)	$(15/2^+) \rightarrow 11/2^+$	1947.6	1095.6
931.0(5)	4.6(12)	$(23/2^-) \rightarrow (19/2^-)$	3255.5	2324.8
955.5(4)	54(6)	$(13/2) \rightarrow 11/2^+$	2051.1	1095.6
999.3(5)	6.2(16)	$(27/2^-) \rightarrow (23/2^-)$	4254.7	3255.5
1095.6(3)*	–	$11/2^+ \rightarrow 7/2^+$	1095.6	0.0

(^{a}) The number in parenthesis is the error in the last digit, the transition marked with a star was already known [33].

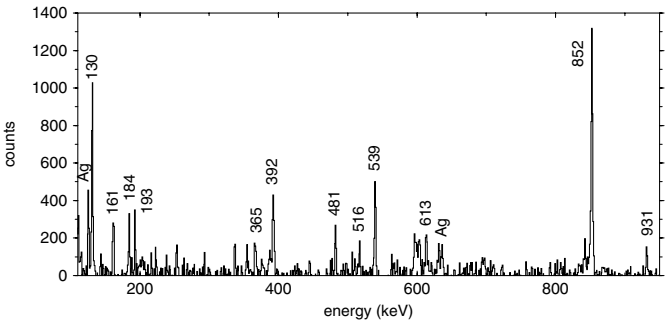

Fig. 8. Spectrum of γ-rays detected in coincidence with two transitions (247 and 1096 keV) of ^{127}Sb, built from the data obtained in the C + U reaction.

It has to be noticed that three levels are proposed at 2378.1 keV, 2378.7 keV keV, and 2379.1 keV, depopulated by three transitions, 183.7 keV, 431.1 keV, and 328.0 keV, respectively. As no other transition has been observed in coincidence with them, we cannot unambiguously establish the number of these levels (three, two or only one) because of the uncertainty on the transition energies. For the level scheme shown in fig. 7, we have chosen to draw three separate levels. This shows evidence of some similarity with ^{125}Sb (the cascades 431-852 and 328-956 of ^{127}Sb can be compared to the cascades 490-904 and 295-1103 of ^{125}Sb, depopulating two different levels 5 keV apart).

In addition, we have measured that the state located at 2325 keV is isomeric with $T_{1/2} = 165 \pm 20$ ns. An $E2$ multipolarity for the 130 keV transition can account for such a value and the isomeric state has been assigned to be $(19/2^-)$, as in ^{123,125}Sb. The properties of the new isomeric states measured in ^{123,125,127}Sb are gathered in table 5.

It is worth pointing out that the $(15/2^-)$ level at 1920 keV, a very long-lived isomeric state with $T_{1/2} = 11$ μs established from β-decay measurements [34], has not been populated in this experiment. Further measurements would be necessary to explain such an unusual feature. Indeed this $(15/2^-)$ level, being yrast, should have been populated in the decay of the higher-spin states.

Table 5. Properties of the isomeric states measured in the present work.

Nucleus	Isomeric state		Isomeric transition	
	Energy (keV)	Half-life (ns)	Energy (keV)	Assigned multipolarity
^{123}Sb	2237.2	110±10	200.4	$E2$
^{125}Sb	2470.1	155±20	145.9	$E2$
^{127}Sb	2324.8	165±20	130.4	$E2$

4 Discussion

To explain the level schemes and the electromagnetic properties of the odd-A $^{115-125}$Sb, a unified-model calculation had been used [35], where single-particle motion and collective degrees of freedom were coupled. The core was described in terms of quadrupole and octupole vibrations, the phonon energies being taken from the neighbouring Sn isotones. A good agreement between theoretical and experimental level schemes up to 3 MeV excitation energy and 11/2 angular momentum had been obtained. In particular, the addition of octupole vibrations was necessary to explain the structure of the lowest $11/2^-$ level which has a rather small single-particle $h_{11/2}$ character. In the following we will discuss to what extent the description of the higher-spin states of the Sb isotopes by the coupling of a single proton to an excited Sn core remains valid.

4.1 First yrast positive-parity states

It has been known for a long time that the value of the angular momentum of the ground state of the odd-A Sb isotopes changes from $I^\pi = 5/2^+$ to $I^\pi = 7/2^+$, between $A = 121$ and $A = 123$. This has been interpreted from the crossing of the $\pi d_{5/2}$ and $\pi g_{7/2}$ sub-shells located just above the $Z = 50$ magic number. This inversion will be discussed in a forthcoming paper [36].

The first-excited state of $^{107-121}$Sb has $I^\pi = 7/2^+$. Whereas this level undoubtedly originates from the $\pi g_{7/2}$ sub-shell for $117 < A < 121$, the nature of the $7/2^+_1$ state measured in $^{107-115}$Sb isotopes has to be discussed. The excitation energies of the $7/2^+_1$, $7/2^+_2$, and $9/2^+_1$ states in odd-A $^{107-121}$Sb isotopes are compared to the ones of the 2^+ states of the corresponding $^{A-1}$Sn cores in fig. 9.

The coupling of $\pi d_{5/2}$ to the 2^+ excitation of the core gives rise to a multiplet of states with spin values ranging from $1/2^+$ to $9/2^+$. One can remark that the $9/2^+_1$ states observed in $^{107-121}$Sb follow very closely the 2^+ core excitation, while the $7/2^+_2$ states in $^{117-121}$Sb are located just below. So in these three isotopes, the $7/2^+_2$ states can be interpreted in terms of the configuration $\pi d_{5/2} \otimes 2^+$.

The behaviour of ^{113}Sb is very peculiar, the energy of its $7/2^+_1$ state is lower than expected from the evolution of the energies measured in $^{117-121}$Sb, while the energy of its $7/2^+_2$ state is higher. This can be easily explained by a strong mixing of the two $7/2^+$ states, which would be degenerated in energy as shown by the crossing

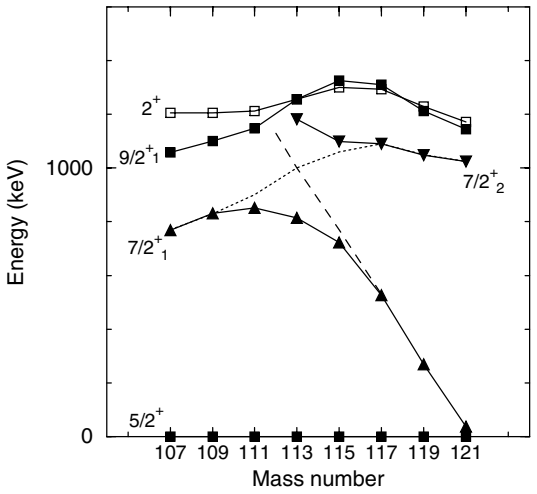

Fig. 9. Evolution of the energies of the $5/2^+_1$, $7/2^+_1$, $7/2^+_2$, and $9/2^+_1$ states in odd-mass $^{107-121}$Sb isotopes, and of the 2^+ states of the corresponding $^{A-1}$Sn cores.

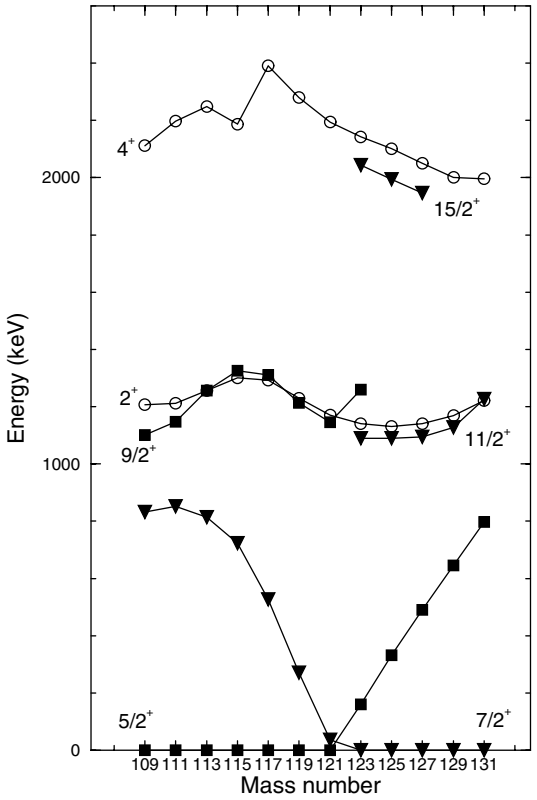

Fig. 10. Evolution of the first yrast positive-parity states in odd-mass ^{A}Sb isotopes, and of the 2^+_1, 4^+_1 states of the corresponding $^{A-1}$Sn cores.

($E \sim 1$ MeV) of the dashed and dotted lines (see fig. 9). It is worth pointing out that the two shifts in energy are found to be the same ($\Delta E = \pm\ 0.18$ MeV) in agreement with a two-state mixing process.

In conclusion, in ^{107,109}Sb, the $7/2^+_1$ state is a member of the multiplet from the $\pi d_{5/2} \otimes 2^+$ configuration, while in ^{111,113,115}Sb, it has a mixed wave function ($\pi g_{7/2}$ and

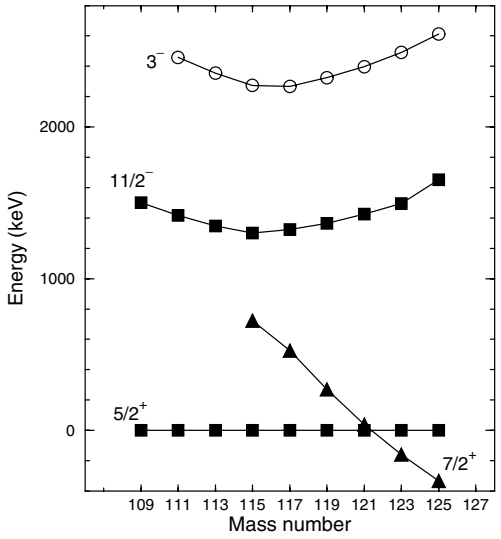

Fig. 11. Evolution of the excitation energy of the first $11/2^-$ state relative to the $5/2^+$ state in the $^{109-125}$Sb isotopes, and of the 3^- octupole state of the corresponding $^{A-1}$Sn cores.

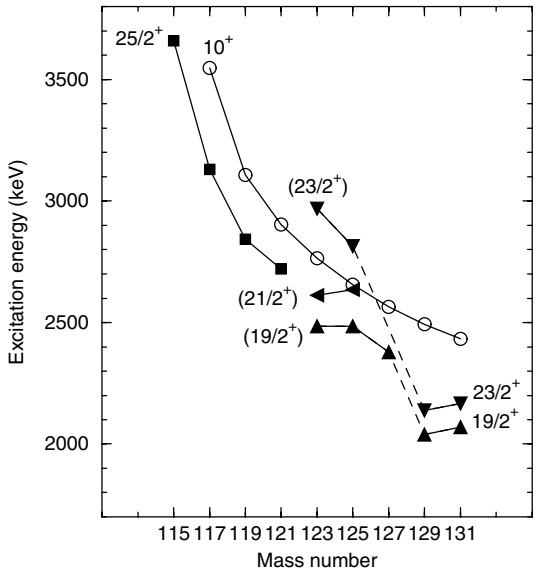

Fig. 12. Evolution of the high-spin positive-parity states in odd-A $^{115-131}$Sb isotopes, and of the 10^+ states of the corresponding $^{A-1}$Sn cores.

$\pi d_{5/2} \otimes 2^+$). Therefore, we have not to look for a strange evolution of the energy of the $\pi g_{7/2}$ sub-shell when the number of neutrons is decreasing in order to explain the behaviour of the energy of the $7/2^+_1$ state in the lighter Sb isotopes.

The systematics of the energies of the first yrast positive-parity states observed in the odd-A $^{109-131}$Sb isotopes is drawn in fig. 10 showing also the evolution of the 2^+_1, 4^+_1 states of the corresponding Sn core. The change of the ground-state configuration between $A = 121$ and $A = 123$ leads to a change of the spin values of the first yrast states. Whereas in $A \leq 121$ the $13/2^+$ state corresponding to the $\pi d_{5/2} \otimes 4^+$ configuration could not be identified in this work, the levels observed at 2044 keV, 1993 keV, and 1948 keV in $A = 123$, 125, and 127, respectively, can be assigned as $15/2^+$ state ($\pi g_{7/2} \otimes 4^+$, see fig. 10).

4.2 Structure of the first $11/2^-$ state

The existence of a $11/2^-$ state in the Sb isotopic series has been proved from the results of one-nucleon transfer (^{3}He, d) reactions on the even Sn isotopes [37]. For $113 \leq A \leq 125$, a state located around 1.4 MeV has been populated with $L = 5$. The low value of the spectroscopic factor indicates that this state has not a pure single-particle configuration, $\pi h_{11/2}$. The addition of octupole vibrations has been necessary to explain its structure [35].

Thanks to the present work, the precise energy of the $11/2^-_1$ state in ^{121,123}Sb isotopes has been measured as well as its decay to the lower states. The evolution of the excitation energy of the first $11/2^-$ state relative to the $5/2^+$ state in the $^{109-125}$Sb isotopes is drawn in fig. 11 showing also the evolution of the 3^- octupole state of the corresponding $^{A-1}$Sn cores. One can notice that the $11/2^-_1$ state is more strongly correlated in energy to the $5/2^+_1$ state than to the $7/2^+_1$ state, even though the latter becomes the ground state (^{123,125}Sb). Therefore in the whole chain, $^{109-125}$Sb, the configuration of the $11/2^-$ state is a strong mixing of the $\pi d_{5/2} \otimes 3^-$ configuration and of the $\pi h_{11/2}$ single-particle excitation. This means that the energy of the $11/2^-$ state of the odd-A Sb isotopes is not a measure of the excitation energy of the $\pi h_{11/2}$ sub-shell, contrary to what is often assumed (see, for instance, the notation given in fig. 12 of ref. [38]).

4.3 Structure of high-spin positive-parity states

Isomeric states with $I^\pi = 25/2^+$ in ^{115,117,119}Sb have been interpreted as a three-particle state with the configuration, $\pi d_{5/2} \otimes \nu h^2_{11/2}$ [39,26]. The systematics of the energies of these $25/2^+$ states is drawn in fig. 12 showing also the evolution of the 10^+ states of the corresponding Sn core. One can notice that the new 2721 keV level of ^{121}Sb we have measured in the present work (see fig. 2 and sect. 3.1) and proposed to be the expected long-lived isomeric $25/2^+$ state from its decay properties, is in good agreement with the evolution in excitation energy.

In the heavier odd-A Sb isotopes, a completely different situation is foreseen. First of all the odd proton occupies another sub-shell, $\pi g_{7/2}$, but the main difference comes from the nature of the nucleons. In the lighter isotopes, both the single proton and the two neutrons are particles, so the state having $I = I_{\max}$ is located at the bottom of the multiplet. In the heaviest isotope, ^{131}Sb, the configuration becomes $\pi g_{7/2} \otimes \nu h^{-2}_{11/2}$. As it contains both particle and holes, the spin of the lowest member of the multiplet corresponds to the perpendicular coupling of the

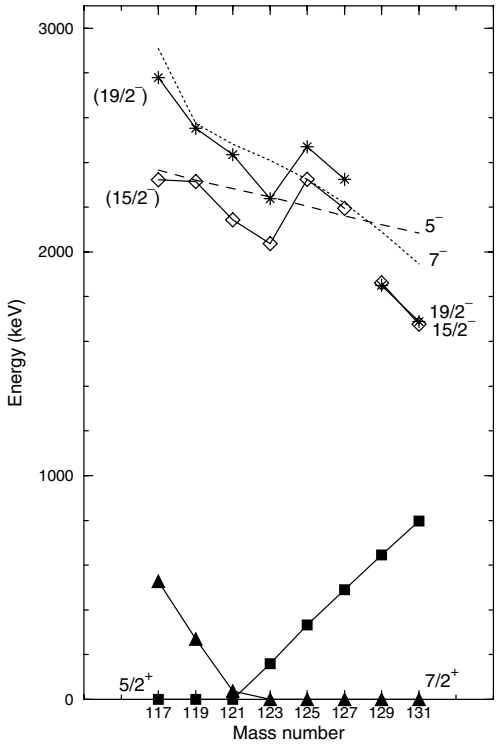

Fig. 13. Evolution of the excitation energy of the $15/2^-$ and $19/2^-$ states in the $^{117-131}$Sb isotopes, and of the 5_1^- and 7_1^- states of the corresponding $^{A-1}$Sn cores.

proton angular momentum and of the two-neutron angular momentum, that is $\sim 19/2^+$, as experimentally observed [10]. For $123 \leq A \leq 129$, the gradual filling of the neutron sub-shell leads to evolutions of the relative energies of the 3qp states. This has been recently discussed in the case of the $\pi g_{9/2} \otimes \nu h_{11/2}^2$ configuration identified in the several odd-A In isotopes [40]. One can notice that the excitation energies of the $(19/2^+)$, $(21/2^+)$, and $(23/2^+)$ states, which are reported in fig. 12, follow the expected trend [40], i) the compression of some energies (for instance, the gap between the $(23/2^+)$ and the $(19/2^+)$ states) and ii) the disappearance of some levels (for instance, the $(21/2^+)$ state is no longer populated in ^{129,131}Sb [9,10]).

4.4 Structure of high-spin negative-parity states

The systematics of the energies of the $15/2^-$ and $19/2^-$ states observed in the odd-A $^{117-131}$Sb isotopes is drawn in fig. 13 showing also the evolution of the 5_1^- and 7_1^- states of the corresponding Sn core. The configuration of these first negative-parity states of Sn isotopes involves one state from the negative-parity intruder sub-shell $\nu h_{11/2}$ and another from one of the positive-parity sub-shells of the $N = 4$ shell, which changes when the number of neutrons increases, as the neutron Fermi level is going up into the $N = 4$ shell. This explains the crossing of the 5_1^- and 7_1^- states between ^{126}Sn and ^{128}Sn. The main configuration of the 5_1^- state of the low-A isotopes is $\nu h_{11/2} \nu s_{1/2}$, while the 7_1^- state of the heaviest Sn isotopes come from the configuration $\nu h_{11/2} \nu d_{3/2}$. In the same way, the $15/2^-$ and $19/2^-$ states of $^{117-131}$Sb isotopes can be interpreted as a break of a neutron pair. This leads to the 3qp configuration, evolving from $\pi d_{5/2} \nu h_{11/2} \nu s_{1/2}$ for the lowest masses to $\pi g_{7/2} \nu h_{11/2} \nu d_{3/2}$ for the heaviest masses. As shown in fig. 13, the energies of the $15/2^-$ and $19/2^-$ states of ^{125}Sb do not follow the gentle trend of the lighter isotopes. This is probably due to the weight of the $\pi d_{5/2}$ orbital in its 3qp configuration. When the neutron number is still increasing, one can expect that the $\pi d_{5/2}$ orbital is no longer involved as its excitation energy becomes too high.

The high-spin part of the level schemes of $^{123-127}$Sb isotopes is dominated by the structure built on the $(19/2^-)$ state (see figs. 3, 5, and 7). From this state up to $(27/2^-, 29/2^-)$ states, cascades of 300–500 keV transitions and several crossover transitions are observed. The energies of the latter being around 1 MeV, the coupling of the 3qp configuration to the quadrupole vibrational excitation of the remaining core can explain the states with spin values between $(19/2^-)$ and $(27/2^-, 29/2^-)$.

At higher spin values, the energies of the transitions are lower and no crossover transitions are measured. These more compressed levels can be interpreted as the break of a second neutron pair which can be expected above 4 MeV excitation energy, the first one being around 2.2 MeV. This leads to the 5qp configuration, evolving from $\pi d_{5/2} \nu h_{11/2}^3 \nu s_{1/2}$ for the low-A Sb isotopes to $\pi g_{7/2} \nu h_{11/2}^3 \nu d_{3/2}$ for the heaviest masses. It is worth pointing out that the ν^4 configurations have not yet been measured in the Sn nuclei with $A \geq 118$, therefore these high-spin structures in Sb isotopes would be the first manifestation of the breaking of two neutron pairs in the Sn cores.

5 Conclusion

Thanks to the high efficiency of the EUROBALL III and IV arrays, new band structures have been identified in the ^{121,123,125,127}Sb nuclei. These isotopes have been produced as fission fragments in three reactions induced by heavy ions: ^{12}C + ^{238}U at 90 MeV bombarding energy, ^{18}O + ^{208}Pb at 85 MeV, and ^{31}P + ^{176}Yb at 152 MeV. The use of the fission-fragment detector, SAPhIR, has allowed us to identify new isomeric states in ^{123,125,127}Sb. All the excited states observed in these Sb nuclei have been interpreted in terms of a single proton coupled to Sn core excitations, either quadrupole and octupole vibrations for the levels with excitation energy below 2 MeV or neutron pair breakings involving both the $\nu h_{11/2}$ sub-shell and the $N = 4$ orbitals. The occupancy of the different proton orbitals lying above $Z = 50$ has been examined. The results of this work confirm the important role played by the $\pi d_{5/2}$ and $\pi g_{7/2}$ orbitals in the structure of the Sb isotopes with $A \geq 113$. As for the lighter isotopes, the first $7/2^+$ state is not due to a single proton in the $\pi g_{7/2}$ orbital but it is a member of the multiplet from the $\pi d_{5/2} \otimes 2^+$ configuration. The $\pi h_{11/2}$ sub-shell does not give rise to a

pure single-proton state at excitation energy below 2 MeV, the main configuration of the first $11/2^-$ state has been assigned to be the $\pi d_{5/2} \otimes 3^-$ coupling, as its excitation energy remains strongly correlated to the $\pi d_{5/2}$ orbital up to $A = 125$. This has to be taken into account when analyzing the energy of the single-proton states predicted by various theoretical calculations. Lastly, many excited states have been discussed in terms of one proton located in the $\pi d_{5/2}$ or $\pi g_{7/2}$ sub-shell coupled to broken neutron pairs. They could be used to test effective neutron-proton interactions in shell model calculations.

The EUROBALL project was a collaboration among France, the United Kingdom, Germany, Italy, Denmark and Sweden. The EUROBALL III experiment has been performed under U.E. contract (ERB FHGECT 980 110) at Legnaro. The EUROBALL IV experiment has been supported in part by the EU under contract HPRI-CT-1999-00078 (EUROVIV). This work was partly supported by the Bulgarian Academy of Sciences - CNRS collaboration agreement under contract No. 16946. S.L. acknowledges financial support provided by the French Institute in Sofia and A.M. by the IN2P3. We thank the crews of the tandem of Legnaro and of the Vivitron. We are very indebted to M.-A. Saettle for preparing the Yb and Pb targets, P. Bednarczyk, J. Devin, J.-M. Gallone, P. Médina, and D. Vintache for their help during the EUROBALL IV experiments.

References

1. R.E. Shroy *et al.*, Phys. Rev. C **19**, 1324 (1979).
2. W.F. Piel *et al.*, Phys. Rev. C **31**, 456 (1985).
3. J. Bron *et al.*, Nucl. Phys. A **318**, 335 (1979).
4. H. Schnare *et al.*, Phys. Rev. C **54**, 1598 (1996).
5. D.R. LaFosse *et al.*, Phys. Rev. C **50**, 1819 (1997).
6. V.P. Janzen *et al.*, Phys. Rev. Lett. **70**, 1065 (1993).
7. R.S. Chakrawarthy, R.G. Pillay, Phys. Rev. C **54**, 2319 (1996).
8. D.R. LaFosse *et al.*, Phys. Rev. C **56**, 760 (1997).
9. J. Genevey *et al.*, Phys. Rev. C **67**, 054312 (2003).
10. J. Genevey *et al.*, Eur. Phys. J. A **9**, 191 (2000).
11. W. Urban *et al.*, Phys. Rev. C **62**, 027301 (2000).
12. J. Simpson, Z. Phys. A **358**, 139 (1997).
13. J. Eberth *et al.*, Nucl. Instrum. Methods A **369**, 135 (1996).
14. G. Duchêne *et al.*, Nucl. Instrum. Methods A **432**, 90 (1999).
15. Ch. Theisen, Euro14 sorting package, unpublished.
16. D. Radford, Nucl. Instrum. Methods A **361**, 297; 306 (1995).
17. I. Deloncle, M.-G. Porquet, M. Dziri-Marcé, Nucl. Instrum. Methods A **357**, 150 (1995).
18. Ch. Theisen *et al.*, *Proceedings of the 2nd International Workshop on Nuclear Fission and Fission Product Spectroscopy, Seyssins, France, April 1998*, AIP Conf. Proc. **447**, 143 (1998).
19. M.A.C. Hotchkis *et al.*, Nucl. Phys. A **530**,111 (1991).
20. M.G. Porquet *et al.*, Acta Phys. Polon. B **27**, 179 (1996).
21. M. Houry *et al.*, Eur. Phys. J. A **6**, 43 (1999).
22. M. Houry, Thèse de Doctorat de l'Université Paris XI, Orsay (January 2000).
23. M.G. Porquet, Int. J. Mod. Phys. E **13**, 29 (2004).
24. R. Lucas *et al.*, Eur. Phys. J. A **15**, 315 (2002).
25. W. Urban *et al.*, Nucl. Instrum. Methods A **365**, 596 (1995).
26. S. Lunardi *et al.*, Z. Phys. A **328**, 487 (1987).
27. T. Tamura, Nucl. Data Sheets **90**, 107 (2000).
28. S. Ohya, T. Tamura, Nucl. Data Sheets **70**, 531 (1993).
29. M.G. Porquet *et al.*, Eur. Phys. J. A **18**, 25 (2003).
30. J. Katakura, Nucl. Data Sheets **86**, 955 (1999).
31. M.G. Porquet *et al.*, *Proton orbitals and rotational structures in the neutron-rich* $^{111-117}$*Ag isotopes*, in preparation.
32. M.G. Porquet *et al.*, unpublished.
33. K. Kitao, M. Oshima, Nucl. Data Sheets **77**, 1 (1996).
34. K. E. Apt, W.B. Walters, Phys. Rev. C **9**, 310 (1974).
35. G. Vanden Berghe, K. Heyde, Nucl. Phys. A **163**, 478 (1971).
36. M.-G. Porquet, S. Péru, M. Girod, in preparation.
37. M. Conjeaud, S. Harar, Y. Cassagnou, Nucl. Phys. A **117**, 449 (1968).
38. J. Shergur *et al.*, Phys. Rev. C **65**, 034313 (2002).
39. J. Bron *et al.*, Nucl. Phys. A **279**, 365 (1977).
40. M.G. Porquet *et al.*, Eur. Phys. J. A **20**, 245 (2004).